Int. J. Heat Mass Transfer. Vol. 30, No. 10, pp. 2073–2082, 1987
Printed in Great Britain

0017-9310/87 $3.00 + 0.00
Pergamon Journals Ltd.

Transient conjugated forced convection in ducts with periodically varying inlet temperature

R. M. COTTA, M. D. MIKHAILOV† and M. N. ÖZIŞIK
Mechanical and Aerospace Engineering Department, North Carolina State University, Rayleigh, NC 27695-7910, U.S.A.

(*Received* 1 *September* 1986)

Abstract—Transient forced convection for slug flow inside parallel-plate channels and circular ducts including conjugation to the walls is solved analytically and exactly for periodic variation of the inlet temperature. The periodic solution to the problem involved eigenfunctions and eigenvalues of a complex eigenvalue problem. The complex eigenvalue problem is solved by modifying the recently advanced Count Method, and benchmark results are presented for the eigenvalues in tabular form. The amplitude and phase lag of oscillations with respect to the conditions at the inlet are determined for the wall temperature, fluid bulk temperature and heat flux. The results for the cases of both parallel-plate channels and circular ducts are presented in the graphical form as a function of the axial position for different values of the parameters signifying the rate of energy storage in the walls. The effects of walls on damping the amplitude and altering the phase of temperature and heat flux oscillations along the duct are investigated.

INTRODUCTION

UNSTEADY forced convection in ducts with periodic variation of the inlet condition is of interest in the control of heat exchanger equipment. For most engineering applications, the initial transients are neglected and the periodic, quasi-stationary solution is used to predict the response of the control device to periodic disturbances. As demonstrated in the review works, by Kalinin and Dreitser [1] and Kakaç and Yener [2], the available work in this area is still very limited. The principal difficulty in the analysis of such problems has been the solution of the resulting complex eigenvalue problem. It appears that, Sparrow and de Farias [3] made the first attempt to evaluate the eigenvalues of the complex transcendental equation associated with the problem of forced slug flow in a parallel-plate duct with conjugation to the walls. Their analysis resulted in the solution of a system of two non-linear equations for the determination of the eigenvalues. A non-documented trial and error procedure was employed for the numerical evaluation of the real and imaginary parts of the eigenvalues. Since the whole spectrum of eigenvalues could not be predicted, some computational difficulties were encountered by following this approach. Kakaç and Yener [2, 4] considered a parabolic velocity profile for flow inside a parallel-plate channel and provided a formal solution for the periodic temperature; but, as the resulting complex eigenvalue problem could not be solved, an experimental technique was utilized to estimate the first eigenvalue.

In the present work we further advance the analysis of ref. [3] by considering transient forced convection in both parallel-plate channels and circular ducts with conjugation to the walls, and subjected to a periodic variation of the inlet temperature. We modify the recently advanced Count Method [5] to adopt for the solution of the complex transcendental equation and present benchmark results for the eigenvalues.

PROBLEM FORMULATION

We consider laminar forced convection inside parallel-plate channels and circular ducts, subjected to periodic time variation in the inlet temperature. We account for conjugation to the wall by balancing the heat transfer rate at the wall surface to the rate of energy storage in the wall. Physical properties are constant and viscous dissipation is negligible. Then the mathematical formulation of the problem is taken as

$$\frac{\partial T(r,z,t)}{\partial t}+u\frac{\partial T(r,z,t)}{\partial z}=\alpha\frac{1}{r^n}\frac{\partial}{\partial r}\left(r^n\frac{\partial T(r,z,t)}{\partial r}\right),$$

$$\text{in}\quad 0<r<r_1,\quad z>0,\quad t>0 \qquad (1a)$$

where

$$n=\begin{cases}0, & \text{for parallel-plate duct}\\ 1, & \text{for circular tube}\end{cases}$$

with the inlet condition given as

$$T(r,0,t)=T_0+\Delta T_0\,e^{i\omega t} \qquad (1b)$$

and the boundary conditions as

† Permanent address: Applied Mathematics Center, Sofia, Bulgaria.

NOMENCLATURE

$A_b(z), A_h(z), A_w(z)$	amplitudes for bulk temperature, heat flux, and wall temperature, respectively
a^*, b^*	defined by equations (2a) and (2b)
a_0, b_0	defined by equation (10b)
a_1, b_1	defined by equation (14a)
c, d	defined by equation (10c)
c_p, c_w	specific heat of fluid and wall, respectively
k	thermal conductivity of fluid
l_w	wall thickness
r	radial or normal coordinate
r_1	radius of circular duct or half the spacing between parallel plates
R	dimensionless normal coordinate, r/r_1
$T(r, z, t)$	fluid temperature
$T_w(z, t)$	wall temperature
T_0	mean valve of inlet temperature cycle
ΔT_0	amplitude of inlet oscillations
u	flow velocity
Z	dimensionless axial coordinate, $\alpha z/ur_1^2$.

Greek symbols

α	thermal diffusivity of fluid
γ, δ	real and imaginary part of eigenvalue, respectively
λ	complex eigenvalue
ρ, ρ_w	fluid and wall density, respectively
ω	frequency of oscillations
Ω	dimensionless frequency of oscillations, $\omega r_1^2/\alpha$
τ	dimensionless time, $\alpha t/r_1^2$
θ	dimensionless temperature, $(T-T_0)/\Delta T_0$
$\phi_b(z), \phi_h(z), \phi_w(z)$	phase lags for bulk temperature, heat flux and wall temperature, respectively.

$$\left.\frac{\partial T(r,z,t)}{\partial r}\right|_{r=0} = 0 \tag{1c}$$

$$-k\left.\frac{\partial T(r,z,t)}{\partial r}\right|_{r=r_1} = \rho_w c_w l_w \frac{\partial T_w(z,t)}{\partial t} \tag{1d}$$

$$T(r_1, z, t) = T_w(z, t). \tag{1e}$$

Since we are seeking the periodic solution only, there is no need for the initial condition.

We now assume the slug flow model by setting u = constant, and introduce the following dimensionless quantities:

$$R = \frac{r}{r_1}, \quad \text{dimensionless normal coordinate}$$

$$Z = \frac{\alpha z}{ur_1^2}, \quad \text{dimensionless axial coordinate}$$

$$\theta(R, Z, \tau) = \frac{T(r,z,t)-T_0}{\Delta T_0}, \quad \text{dimensionless temperature}$$

$$\tau = \frac{\alpha t}{r_1^2}, \quad \text{dimensionless time}$$

$$\Omega = \frac{\omega r_1^2}{\alpha}, \quad \text{dimensionless frequency of the periodic inlet temperature.}$$

In addition we define the following two dimensionless parameters to characterize the effects of wall capacitance to heat transfer:

$$a^* = \frac{\rho c_p r_1}{\rho_w c_w l_w} \tag{2a}$$

$$b^* = \frac{\Omega}{a^*} = \frac{\omega r_1 \rho_w c_w l_w}{k}. \tag{2b}$$

Equation (1e) is introduced into equation (1d), and then problem (1) is expressed in the dimensionless form by utilizing the above dimensionless quantities. We obtain

$$\frac{\partial\theta(R,Z,\tau)}{\partial\tau} + \frac{\partial\theta(R,Z,\tau)}{\partial Z} = \frac{1}{R^n}\frac{\partial}{\partial R}\left(R^n \frac{\partial\theta(R,Z,\tau)}{\partial R}\right),$$

$$\text{in} \quad 0 < R < 1, \quad Z > 0, \quad \tau > 0 \tag{3a}$$

$$\theta(R, 0, \tau) = e^{i\Omega\tau} \tag{3b}$$

$$\left.\frac{\partial\theta(R,Z,\tau)}{\partial R}\right|_{R=0} = 0 \tag{3c}$$

$$a^*\left.\frac{\partial\theta(R,Z,\tau)}{\partial R}\right|_{R=1} + \frac{\partial\theta(1,Z,\tau)}{\partial\tau} = 0 \tag{3d}$$

and the initial condition is not needed for the periodic solution.

METHOD OF SOLUTION

To develop a periodic solution to problem (3), we make the following substitution

$$\theta(R, Z, \tau) = \tilde{\theta}(R, Z)\, e^{i\Omega(\tau - Z)} \tag{4}$$

which results in the following problem for $\tilde{\theta}(R, Z)$:

$$\frac{\partial\tilde{\theta}(R,Z)}{\partial Z} = \frac{1}{R^n}\frac{\partial}{\partial R}\left(R^n \frac{\partial\tilde{\theta}(R,Z)}{\partial R}\right),$$

$$\text{in} \quad 0 < R < 1, \quad Z > 0 \tag{5a}$$

with the inlet and boundary conditions given by

$$\tilde{\theta}(R, 0) = 1 \tag{5b}$$

$$\left.\frac{\partial\tilde{\theta}(R,Z)}{\partial R}\right|_{R=0}=0 \tag{5c}$$

$$a^*\left.\frac{\partial\tilde{\theta}(R,Z)}{\partial R}\right|_{R=1}+\mathrm{i}\Omega\tilde{\theta}(1,Z)=0. \tag{5d}$$

The formal solution to problem (5) is obtained by the integral transform technique [6] as

$$\tilde{\theta}(R,Z)=2\sum_{j=1}^{\infty}\frac{\exp(-\lambda_j^2 Z)}{\lambda_j\left\{1+\dfrac{2m}{\mathrm{i}b^*}+\left(\dfrac{\lambda_j}{\mathrm{i}b^*}\right)^2\right\}}R^m\frac{J_{-m}(\lambda_j R)}{J_{1-m}(\lambda_j)} \tag{6a}$$

where

$$m=\frac{1-n}{2}=\begin{cases}1/2, & \text{for parallel-plate duct}\\ 0, & \text{for circular tube}\end{cases}$$

and λ_js are the roots of the following complex transcendental equation:

$$\mathrm{i}b^*J_{-m}(\lambda)-\lambda J_{1-m}(\lambda)=0 \tag{6b}$$

which is obtained from the related complex eigenvalue problem.

Once the solution is available for $\tilde{\theta}(R,Z)$, the *wall temperature* $\theta_w(Z,\tau)$ is obtained from equation (4)

$$\theta_w(Z,t)\equiv\theta(1,Z,\tau)=\tilde{\theta}(1,Z)\mathrm{e}^{\mathrm{i}\Omega(\tau-Z)} \tag{7}$$

the dimensionless *fluid bulk temperature* $\theta_b(Z,\tau)$ is determined from its definition as

$$\theta_b(Z,\tau)=(n+1)\int_0^1 R^n\theta(R,Z,\tau)\,\mathrm{d}R$$

$$=4(1-m)\left\{\sum_{j=1}^{\infty}\frac{\exp(-\lambda_j^2 Z)}{\lambda_j^2\left[1+\dfrac{2m}{\mathrm{i}b^*}+\left(\dfrac{\lambda_j}{\mathrm{i}b^*}\right)^2\right]}\right\}\mathrm{e}^{\mathrm{i}\Omega(\tau-Z)} \tag{8}$$

and the dimensionless *wall heat flux* $Q_w(Z,\tau)$ is obtained as

$$Q_w(Z,\tau)=-\left.\frac{\partial\theta(R,Z,\tau)}{\partial R}\right|_{R=1}$$

$$=2\left\{\sum_{j=1}^{\infty}\frac{\exp(-\lambda_j^2 Z)}{1+\dfrac{2m}{\mathrm{i}b^*}+\left(\dfrac{\lambda_j}{\mathrm{i}b^*}\right)^2}\right\}\mathrm{e}^{\mathrm{i}\Omega(\tau-Z)}. \tag{9}$$

The eigenvalue problem being complex, both the eigenvalues and eigenfunctions are complex quantities. Therefore, we separate them into real and imaginary parts as

$$\lambda_j=\gamma_j+\mathrm{i}\delta_j \tag{10a}$$

$$J_{-m}(\lambda_j)=a_0(\gamma,\delta)+\mathrm{i}b_0(\gamma,\delta) \tag{10b}$$

$$J_{1-m}(\lambda_j)=c(\gamma,\delta)+\mathrm{i}d(\gamma,\delta) \tag{10c}$$

where $\mathrm{i}=\sqrt{-1}$. Then $Q_w(Z,\tau)$, $\theta_b(Z,\tau)$ and $\theta_w(Z,\tau)$ are written in polar coordinates as

$$Q_w(Z,\tau)=A_h(Z)\exp[\mathrm{i}(\Omega\tau+\phi_h(Z))] \tag{11a}$$

$$\theta_b(Z,\tau)=A_b(Z)\exp[\mathrm{i}(\Omega\tau+\phi_b(Z))] \tag{11b}$$

$$\theta_w(Z,\tau)=A_w(Z)\exp[\mathrm{i}(\Omega\tau+\phi_w(Z))] \tag{11c}$$

where the various amplitudes $A_h(Z)$, $A_b(Z)$, $A_w(Z)$ and the phase lags $\phi_h(Z)$, $\phi_b(Z)$, $\phi_w(Z)$ are given by

$$A_h(Z)=\left\{\left[2\sum_{j=1}^{\infty}C_j\mathrm{e}^{-\gamma_j^* Z}F_j(Z)\right]^2+\left[2\sum_{j=1}^{\infty}C_j\mathrm{e}^{-\gamma_j^* Z}G_j(Z)\right]^2\right\}^{1/2} \tag{12a}$$

$$\phi_h(Z)=\tan^{-1}\left\{\frac{\sum_{j=1}^{\infty}C_j\mathrm{e}^{-\gamma_j^* Z}G_j(Z)}{\sum_{j=1}^{\infty}C_j\mathrm{e}^{-\gamma_j^* Z}F_j(Z)}\right\} \tag{12b}$$

$$A_b(Z)=\left\{\left[4(1-m)\sum_{j=1}^{\infty}C_j^*\mathrm{e}^{-\gamma_j^* Z}F_j^*(Z)\right]^2+\left[4(1-m)\sum_{j=1}^{\infty}C_j^*\mathrm{e}^{-\gamma_j^* Z}G_j^*(Z)\right]^2\right\}^{1/2} \tag{12c}$$

$$\phi_b(Z)=\tan^{-1}\left\{\frac{\sum_{j=1}^{\infty}C_j^*\mathrm{e}^{-\gamma_j^* Z}G_j^*(Z)}{\sum_{j=1}^{\infty}C_j^*\mathrm{e}^{-\gamma_j^* Z}F_j^*(Z)}\right\} \tag{12d}$$

$$A_w(Z)=\left\{\left[2\sum_{j=1}^{\infty}C_j^{**}\mathrm{e}^{-\gamma_j^* Z}F_j^{**}(Z)\right]^2+\left[2\sum_{j=1}^{\infty}C_j^{**}\mathrm{e}^{-\gamma_j^* Z}G_j^{**}(Z)\right]^2\right\}^{1/2} \tag{12e}$$

$$\phi_w(Z)=\tan^{-1}\left\{\frac{\sum_{j=1}^{\infty}C_j^{**}\mathrm{e}^{-\gamma_j^* Z}G_j^{**}(Z)}{\sum_{j=1}^{\infty}C_j^{**}\mathrm{e}^{-\gamma_j^* Z}F_j^{**}(Z)}\right\} \tag{12f}$$

where

$$C_j=\frac{b^{*2}}{(b^{*2}-\gamma_j^2+\delta_j^2)^2+4(mb^*+\gamma_j\delta_j)^2} \tag{13a}$$

$$F_j(Z)=[(b^{*2}-\gamma_j^2+\delta_j^2)\cos(\delta_j^* Z)+2(mb^*+\gamma_j\delta_j)\sin(\delta_j^* Z)]\cdot\cos(\Omega Z)+[2(mb^*+\gamma_j\delta_j)\cos(\delta_j^* Z)-(b^{*2}-\gamma_j^2+\delta_j^2)\sin(\delta_j^* Z)]\cdot\sin(\Omega Z) \tag{13b}$$

$$G_j(Z)=[2(mb^*+\gamma_j\delta_j)\cos(\delta_j^* Z)-(b^{*2}-\gamma_j^2+\delta_j^2)\sin(\delta_j^* Z)]\cdot\cos(\Omega Z)-[(b^{*2}-\gamma_j^2+\delta_j^2)\cos(\delta_j^* Z)+2(mb^*+\gamma_j\delta_j)\sin(\delta_j^* Z)]\cdot\sin(\Omega Z) \tag{13c}$$

$$C_j^*=\frac{C_j}{(\gamma_j^2+\delta_j^2)^2} \tag{13d}$$

$$F_j^*(Z)=\gamma_j^*F_j(Z)+\delta_j^*G_j(Z) \tag{13e}$$

$$G_j^*(Z)=\gamma_j^*G_j(Z)-\delta_j^*F_j(Z) \tag{13f}$$

$$C_j^{**} = \frac{C_j}{a_1^2 + b_1^2} \tag{13g}$$

$$F_j^{**}(Z) = (a_0 a_1 + b_0 b_1) F_j(Z) - (b_0 a_1 - b_1 a_0) G_j(Z) \tag{13h}$$

$$G_j^{**}(Z) = (b_0 a_1 - b_1 a_0) F_j(Z) + (a_0 a_1 + b_0 b_1) G_j(Z) \tag{13i}$$

$$\gamma_j^* = \gamma_j^2 - \delta_j^2; \quad \delta_j^* = 2\gamma_j \delta_j \tag{13j, k}$$

in addition, a_1 and b_1 are the real and imaginary parts of $-\lambda J_{1-m}(\lambda)$, that is

$$-\lambda J_{1-m}(\lambda) = a_1 + ib_1 \tag{14a}$$

and are determined as

$$a_1 = \delta_j d - \gamma_j c \quad \text{and} \quad b_1 = -(\gamma_j d + \delta_j c). \tag{14b, c}$$

Therefore, if the real and imaginary parts γ_j and δ_j of the complex eigenvalues are available, numerical values of the amplitudes and phase lags are readily determined from the expressions given previously. Therefore, our task is now reduced to the computation of γ_j and δ_j.

COMPUTATION OF EIGENVALUES

By introducing equations (10b) and (14a) into equation (6b), the complex transcendental equation is transformed to the following system of two coupled transcendental equations obtained from the real and imaginary parts, respectively:

$$-b^* b_0(\gamma, \delta) + a_1(\gamma, \delta) = 0 \tag{15a}$$

$$b^* a_0(\gamma, \delta) + b_1(\gamma, \delta) = 0. \tag{15b}$$

Following the formalism of the Count Method, these equations resulting from the real and imaginary parts of the transcendental equation are rewritten, respectively, as

$$f_1(\gamma; \delta) \equiv b^* - \frac{a_1(\gamma, \delta)}{b_0(\gamma, \delta)} = 0 \tag{16a}$$

$$f_2(\gamma; \delta) \equiv b^* + \frac{b_1(\gamma, \delta)}{a_0(\gamma, \delta)} = 0. \tag{16b}$$

In this formalism, we imply that, the first argument γ in the functions $f_i(\gamma; \delta)$, $i = 1$ or 2, refers to the *unknown variable* and the second argument δ refers to the *parameter*. Furthermore, the roots of $b_0(\gamma, \delta)$ and $a_0(\gamma, \delta)$ in equations (16) provide the points of singularity in the behavior of functions $f_1(\gamma, \delta)$ and $f_2(\gamma, \delta)$, respectively. For the Count Method to be applicable for equations (16), the functions $f_1(\gamma; \delta)$ and $f_2(\gamma; \delta)$ should exhibit a monotonic variation inside each interval defined by two consecutive singular points. For the present problem, the functions $f_1(\gamma; \delta)$ and $f_2(\gamma; \delta)$ decrease monotonically with increasing γ in each of such intervals. Then the number of roots of $f_1(\gamma; \delta)$ or $f_2(\gamma; \delta)$ lying below a certain guess value of $\tilde{\gamma}$, for a specified δ, can readily be determined since there should be one root in each of such intervals, except in the interval in which $\tilde{\gamma}$ is chosen. In this last interval, the sign of the function $f_1(\tilde{\gamma}, \delta)$ or $f_2(\tilde{\gamma}, \delta)$, for the chosen value of $\tilde{\gamma}$, establishes whether $\tilde{\gamma}$ contains the root in the last interval or not. By merely examining the sign of the function $f_1(\tilde{\gamma}, \delta)$ or $f_2(\tilde{\gamma}, \delta)$, an upper and a lower limit is established for the value of γ. Then a bisection procedure can be implemented to converge, at any desired accuracy, to the proper value of γ corresponding to the order of the eigenvalue searched.

The same principles apply, if, alternatively, δ is chosen as the *unknown variable* and γ the parameter. For this case the equations associated with the imaginary and real parts are written, respectively, as

$$f_3(\delta; \gamma) \equiv b^* + \frac{b_1(\delta, \gamma)}{a_0} = 0 \tag{17a}$$

$$f_4(\delta; \gamma) \equiv -b^* + \frac{a_1(\delta, \gamma)}{b_0} = 0 \tag{17b}$$

where δ is the unknown variable and γ is the parameter. In the equation for $f_4(\delta; \gamma)$, the sign is changed on the right-hand side, for convenience, in order to maintain monotonically decreasing property for all of the four equations.

In principle, the computations can be performed either using the pair of functions '$f_1(\gamma; \delta)$ and $f_3(\delta; \gamma)$' associated with the real and imaginary parts, or the pair of functions '$f_2(\gamma; \delta)$ and $f_4(\delta; \gamma)$' associated with the imaginary and real parts. It is possible that one of these pairs might not converge for the whole spectrum of eigenvalues being searched. Then, for such a situation, switching to the other pair of equations alleviates the convergence difficulty. For the specific problems of a parallel-plate channel and circular duct considered here, the functions $f_3(\delta; \gamma)$ and $f_4(\delta; \gamma)$, for a given guess value of γ, have only one root in the interval $0 \leqslant \delta < \infty$. Therefore, one needs to study only the sign of $f_3(\delta; \gamma)$ or $f_4(\delta; \gamma)$ in order to find the upper and lower bounds for δ, and then use the bisection procedure to converge to the proper value of δ.

The computational process for the determination of γ and δ, in general, is similar to the Count Method [5], but, in the present problem two non-linear equations are to be satisfied. Therefore, the iterations are continued until covergence is achieved for both γ and δ.

In some very special situations, if the convergence by the bisection process is found to be very slow, the unconverged results can provide an excellent first guess for the roots. Once such a good approximation is available for the roots, a standard efficient subroutine package for solving the system of non-linear equations can be used to converge rapidly to the exact values of the roots.

We summarize below the algorithm we used for calculating the eigenvalues of the complex eigenvalue problem encountered in the present problem.

STEP 1: Make a guess for $\tilde{\gamma}_j$ inside the interval defined by the roots of $b_0(\gamma, 0)$ or $a_0(\gamma, 0)$, if the equation for $f_1(\gamma; \delta)$ or $f_2(\gamma; \delta)$ is used, respectively.

STEP 2: Guess $\tilde{\delta}_j$. Taking zero as a lower bound study the signs of either $f_3(\delta; \gamma)$ or $f_4(\delta; \gamma)$ until a pair of upper and lower bounds is established. Apply the bisection procedure until desired tolerancy is reached in converging to δ_j.

STEP 3: Evaluate, by any reliable conventional procedure, the roots of $b_0(\gamma; \delta_j)$ or $a_0(\gamma; \delta_j)$ to redefine singular points. In general the roots of $b_0(\gamma; 0)$ or $a_0(\gamma; 0)$ provide a sufficiently good first guess.

STEP 4: Guess $\tilde{\gamma}_j$ inside the desired interval of updated singular points. Taking the left extreme of the interval, start the 'counting' procedure and study the signs of either $f_1(\gamma; \delta)$ or $f_2(\gamma; \delta)$ until a pair of upper and lower bounds is established. Apply the bisection procedure until desired tolerancy is achieved in converging to $\tilde{\gamma}_j$.

STEP 5: Go to Step 2 and repeat procedure until both γ_j and δ_j converge to the desired accuracy. In general, previous values of γ_j and δ_j can now be used as guesses in Steps 2 and 4 to speed up the procedure, as well as previous roots of $b_0(\gamma; \delta_j)$ or $a_0(\gamma; \delta_j)$.

STEP 6: If convergence is not achieved, switch systems of equations and restart from Step 1. If convergence is particularly slow, refinement can be obtained by making use of a packed subroutine for the solution of systems of non-linear equations (e.g. IMSL subroutines package), using latest results available as first guesses.

STEP 7: Select next order j and restart procedure from Step 1 using the last successful system of equations.

The present scheme proved to be extremely fast and reliable, since roots cannot be missed and, in general only a few iterations are required to reach several digits of accuracy. Quite rarely, in extremely special situations, one needs to make use of the refinement mentioned in Step 6, which is now itself fast and reliable, since excellent first guesses are provided.

For the special case of slug flow inside a parallel-plate channel and a circular tube, the coefficients a_0, b_0, c and d are given as follows:

Parallel-plate channel

$$a_0(\gamma, \delta) = \cos\gamma \cosh\delta \tag{18a}$$

$$b_0(\gamma, \delta) = -\sin\gamma \sinh\delta \tag{18b}$$

$$c(\gamma, \delta) = \sin\gamma \cosh\delta \tag{18c}$$

$$d(\gamma, \delta) = \cos\gamma \sinh\delta. \tag{18d}$$

Circular duct

$$a_0(\gamma, \delta) = \mathrm{Re}\,[J_0(\lambda)] \tag{19a}$$

$$b_0(\gamma, \delta) = \mathrm{Im}\,[J_0(\lambda)] \tag{19b}$$

$$c(\gamma, \delta) = \mathrm{Re}\,[J_1(\lambda)] \tag{19c}$$

$$d(\gamma, \delta) = \mathrm{Im}\,[J_1(\lambda)] \tag{19d}$$

where the circular duct functions are obtainable from a standard routine for Bessel functions with complex arguments. For the case of a parallel-plate channel, some cancellation of terms is possible in the expressions f_1 and f_2, which results in the exclusion of the imaginary part δ of the eigenvalues in the calculation of the singular points. Therefore, for such a case, the singularities need to be calculated just once and Step 3 can be omitted.

RESULTS AND DISCUSSION

In Tables 1 and 2 we present a systematic tabulation of the first 25 eigenvalues defined by their real and imaginary parts as given in equation (10a) for parallel-plates and circular ducts, respectively. Following ref. [3] we selected the representative values of the parameter b^* in excess of one, namely, $b^* = 1, 2, 5, 10, 20$ and 100. A large number of eigenvalues were determined and calculations were performed for various other values of b^*; but space limitations preclude a more extensive presentation. Table 1, for a parallel-plate channel, is included, since there is some accuracy improvement in comparison to the results in ref. [3], and since the whole spectrum of eigenvalues could not be obtained from that work.

Quantities of practical interest, such as wall temperature, fluid bulk temperature, and wall heat flux, were evaluated. However, we have chosen to present these results in the form of amplitude and time lag of local oscillations with respect to the inlet conditions and plotted them as a function of the axial distance along the duct. Figures 1(a) and (b) show amplitude $A_w(Z)$ and phase lag $\phi_w(Z)$ for the wall temperature for a parallel-plate channel and circular duct, respectively, for the values of $b^* = 2, 5, 10$ and 20. The significance of parameter b^* can be interpreted as the ratio of rate of energy storage at the wall to heat transfer by conduction across the fluid to or from the wall. From Figs. 1(a) and (b) we note that, for large values of b^* the thermal wave has little penetration along the duct, because it decays rapidly with the axial distance. Therefore, oscillations in fluid temperature are damped within a short distance from the inlet because of the large thermal capacity of the walls; and consequently the wall temperature oscillation is drastically reduced. For small values of b^*, the thermal wave penetrates further down along the duct, because wall thermal capacity being small it requires a longer distance for the same amount of heat to be stored in the wall. These same general trends apply for both parallel-plate channels and circular ducts; however, the attenuation of the amplitude seems to be more pronounced in the circular duct and the time lag is somewhat larger. In Figs. 2(a) and (b) we present the amplitude and phase lag of fluid bulk temperature for a parallel-plate channel and a circular duct, respectively. Again, for large values of b^*, the thermal waves are attenuated within a short distance from the inlet. Note that the attenuation for the wall temperature is much stronger than that for the bulk temperature. As

Table 1. First 25 eigenvalues for a parallel-plate channel

j	γ	δ	γ	δ	γ	δ
	$b^* = 1.0$		$b^* = 2.0$		$b^* = 5.0$	
1	0.800453	0.570033	1.173902	0.580817	1.503032	0.308807
2	3.176552	0.321942	3.310593	0.648553	4.209334	0.993579
3	6.287343	0.160303	6.301475	0.327680	6.518534	0.934464
4	9.425990	0.106477	9.429844	0.215240	9.469539	0.583561
5	12.566879	0.079740	12.568455	0.160465	12.582095	0.419923
6	15.708223	0.063746	15.709018	0.128001	15.715379	0.329425
7	18.849706	0.053101	18.850162	0.106497	18.853665	0.271630
8	21.991243	0.045504	21.991529	0.091194	21.993670	0.231353
9	25.132804	0.039810	25.132995	0.079744	25.134402	0.201605
10	28.274378	0.035382	28.274512	0.070853	28.275487	0.178703
11	31.415959	0.031842	31.416056	0.063748	31.416761	0.160511
12	34.557543	0.028945	34.557617	0.057939	34.558142	0.145703
13	37.699131	0.026532	37.699187	0.053101	37.699590	0.133412
14	40.840719	0.024490	40.840763	0.049010	40.841079	0.123042
15	43.982309	0.022740	43.982344	0.045504	43.982596	0.114174
16	47.123899	0.021224	47.123928	0.042467	47.124132	0.106503
17	50.265490	0.019897	50.265514	0.039810	50.265682	0.099801
18	53.407082	0.018726	53.407101	0.037466	53.407241	0.093895
19	56.548673	0.017686	56.548690	0.035382	56.548807	0.088650
20	59.690265	0.016755	59.690279	0.033519	59.690379	0.083962
21	62.831857	0.015917	62.831869	0.031842	62.831955	0.079746
22	65.973449	0.015159	65.973460	0.030325	65.973533	0.075933
23	69.115041	0.014470	69.115051	0.028945	69.115115	0.072470
24	72.256634	0.013840	72.256642	0.027686	72.256698	0.069308
25	75.398226	0.013264	75.398233	0.026532	75.398282	0.066412
	$b^* = 10.0$		$b^* = 20.0$		$b^* = 100.0$	
1	1.554739	0.156705	1.566847	0.078502	1.570639	0.015708
2	4.648546	0.501593	4.699719	0.239423	4.711916	0.047154
3	7.632836	0.966257	7.829583	0.413313	7.853190	0.078694
4	10.129043	1.349910	10.951788	0.613882	10.994457	0.110391
5	12.724169	1.027868	14.052036	0.867322	14.135715	0.142310
6	15.757852	0.745144	17.064149	1.227805	17.276961	0.174520
7	18.872500	0.588971	19.705840	1.598343	20.418191	0.207092
8	22.003891	0.489956	22.250740	1.386067	23.559403	0.240103
9	25.140648	0.420831	25.221905	1.069232	26.700591	0.273635
10	28.279613	0.369487	28.317785	0.877020	29.841752	0.307778
11	31.419642	0.329680	31.441386	0.750583	32.982878	0.342631
12	34.560240	0.297831	34.574092	0.659682	36.123965	0.378304
13	37.701168	0.271725	37.710658	0.590386	39.265003	0.414920
14	40.842298	0.249910	40.849142	0.535397	42.405982	0.452619
15	43.983558	0.231394	43.988686	0.490472	45.546891	0.491562
16	47.124906	0.215471	47.128863	0.452950	48.687714	0.531935
17	50.266313	0.201626	50.269441	0.421060	51.828431	0.573959
18	53.407763	0.189471	53.410284	0.393573	54.969018	0.617894
19	56.549245	0.178714	56.551309	0.369602	58.109439	0.664055
20	59.690749	0.169123	59.692464	0.348492	61.249650	0.712827
21	62.832270	0.160517	62.833712	0.329744	64.389588	0.764691
22	65.973805	0.152752	65.975029	0.312971	67.529166	0.820254
23	69.115350	0.145707	69.116399	0.297869	70.668254	0.880307
24	72.256903	0.139288	72.257810	0.284194	73.806658	0.945901
25	75.398463	0.133414	75.399252	0.271748	76.944069	1.018476

stated previously, the thermal capacity of the wall in the parameter b^* plays an important role in damping the amplitude of temperature oscillations. On the other hand the parameter b^* can also be larger due to the small values of the fluid thermal conductivity; in such cases, less heat is transferred across the fluid to (or from) the wall at each axial location, which in turn represents smaller variations in the bulk and consequently wall temperatures. With the smaller values of b^*, the wall and bulk temperatures are closer, since the information carried by the thermal wave is sensed almost entirely by the wall at the same location. Since we are not considering fluids with very high thermal conductivity such as liquid metals, this interpretation should be taken as a result of the ratio of heat storage at the wall and the heat transferred across the fluid. The geometry has also some effect on the amplitude and phase lag. The amplitudes are

Table 2. First 25 eigenvalues for a circular duct

j	γ	δ	γ	δ	γ	δ
	$b^* = 1.0$		$b^* = 2.0$		$b^* = 5.0$	
1	1.111798	0.861266	1.683410	0.976183	2.333615	0.512700
2	3.841619	0.266392	3.887368	0.566309	4.775688	1.262684
3	7.017084	0.143485	7.022231	0.292886	7.114421	0.863294
4	10.173951	0.098609	10.175495	0.199141	10.191935	0.536559
5	13.323905	0.075194	13.324570	0.151241	13.330463	0.394293
6	16.470743	0.060788	16.471089	0.122027	16.473910	0.313376
7	19.615925	0.051023	19.616128	0.102312	19.617709	0.260615
8	22.760127	0.043965	22.760256	0.088100	22.761235	0.223311
9	25.903701	0.038624	25.903788	0.077363	25.904438	0.195469
10	29.046849	0.034441	29.046911	0.068963	29.047365	0.173864
11	32.189695	0.031076	32.189740	0.062212	32.190070	0.156595
12	35.332319	0.028310	35.332353	0.056666	35.332601	0.142468
13	38.474775	0.025997	38.474802	0.052029	38.474992	0.130694
14	41.617101	0.024033	41.617122	0.048094	41.617272	0.120726
15	44.759325	0.022345	44.759341	0.044713	44.759461	0.112176
16	47.901465	0.020879	47.901479	0.041777	47.901577	0.104762
17	51.043539	0.019594	51.043550	0.039202	51.043631	0.098271
18	54.185557	0.018457	54.185566	0.036927	54.185633	0.092539
19	57.327528	0.017445	57.327536	0.034901	57.327593	0.087440
20	60.469460	0.016539	60.469467	0.033087	60.469515	0.082876
21	63.611359	0.015722	63.611364	0.031451	63.611406	0.078765
22	66.753228	0.014982	66.753233	0.029970	66.753269	0.075043
23	69.895073	0.014308	69.895078	0.028622	69.895109	0.071658
24	73.036897	0.013693	73.036900	0.027390	73.036928	0.068566
25	76.178701	0.013128	76.178704	0.026260	76.178728	0.065730
	$b^* = 10.0$		$b^* = 20.0$		$b^* = 100.0$	
1	2.391580	0.244716	2.401747	0.120771	2.404705	0.024052
2	5.471201	0.616091	5.512216	0.283168	5.519801	0.055256
3	8.404109	1.184718	8.638568	0.462660	8.653290	0.086753
4	10.653160	1.443372	11.762399	0.675219	11.790931	0.118464
5	13.396963	0.959490	14.865637	0.956632	14.930143	0.150431
6	16.493836	0.702539	17.848395	1.395335	18.070109	0.182714
7	19.626631	0.561975	20.283319	1.731004	21.210492	0.215382
8	22.766101	0.471274	22.899372	1.326965	24.351124	0.248512
9	25.907420	0.407070	25.949963	1.019918	27.491914	0.282187
10	29.049339	0.358893	29.069272	0.843682	30.632804	0.316499
11	32.191452	0.321254	32.202741	0.726580	33.773758	0.351549
12	35.333609	0.290958	35.340752	0.641436	36.914750	0.387449
13	38.475752	0.266005	38.480616	0.575958	40.055757	0.424327
14	41.617860	0.245073	41.621348	0.523649	43.196763	0.462329
15	44.759926	0.227247	44.762528	0.480690	46.337751	0.501621
16	47.901951	0.211874	47.903951	0.444659	49.478704	0.542397
17	51.043936	0.198475	51.045512	0.413931	52.619602	0.584888
18	54.185887	0.186689	54.187153	0.387369	55.760423	0.629368
19	57.327805	0.176238	57.328840	0.364149	58.901140	0.676168
20	60.469695	0.166905	60.470553	0.343658	62.041714	0.725698
21	63.611559	0.158519	63.612279	0.325425	65.182096	0.778468
22	66.753401	0.150941	66.754012	0.309088	68.322214	0.835132
23	69.895223	0.144060	69.895746	0.294357	71.461962	0.896544
24	73.037028	0.137782	73.037479	0.281002	74.601178	0.963851
25	76.178816	0.132032	76.179209	0.268833	77.739600	1.038647

somewhat smaller for a circular tube than for a parallel-plate channel, and phase lags larger.

Figures 3(a) and (b) show the amplitude and phase lag for the wall heat flux, for a parallel-plate channel and a circular tube, respectively. For very small axial distances from the inlet, the amplitude of the wall heat flux is larger with larger values of b^*, since the temperature gradients are steeper due to the pronounced attenuation in the wall temperature. At large distances from the inlet, the amplitude of the heat flux decreases with increasing b^*. The amplitudes are somewhat smaller for a circular tube than for a parallel-plate channel.

Figure 4 shows the effects of the parameter a^*, characterizing the ratio of heat capacities of fluid to wall, on the amplitude and phase lag of bulk temperature for flow inside a circular tube. As pointed out in ref. [3], for the flow of a gas inside a duct with

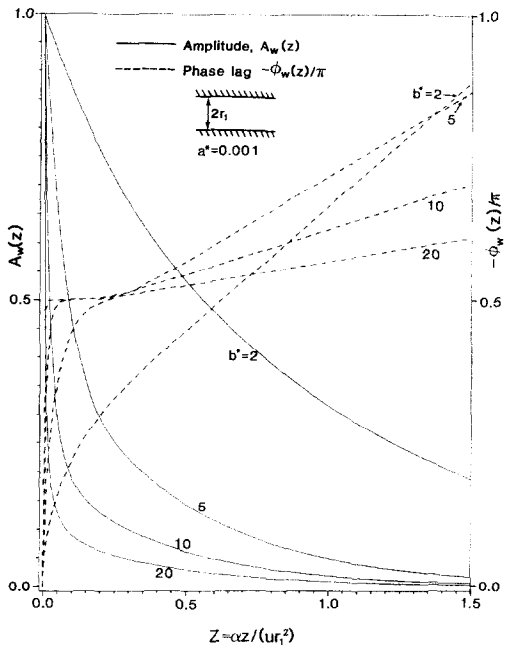

FIG. 1(a). Amplitude and phase lag for wall temperature as a function of the axial distance in a parallel-plate channel for various values of b^*.

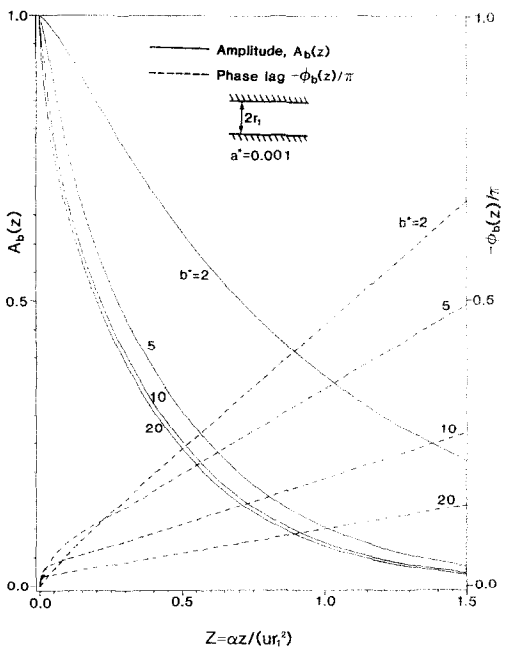

FIG. 2(a). Amplitude and phase lag for bulk temperature as a function of the axial distance in a parallel-plate channel for various values of b^*.

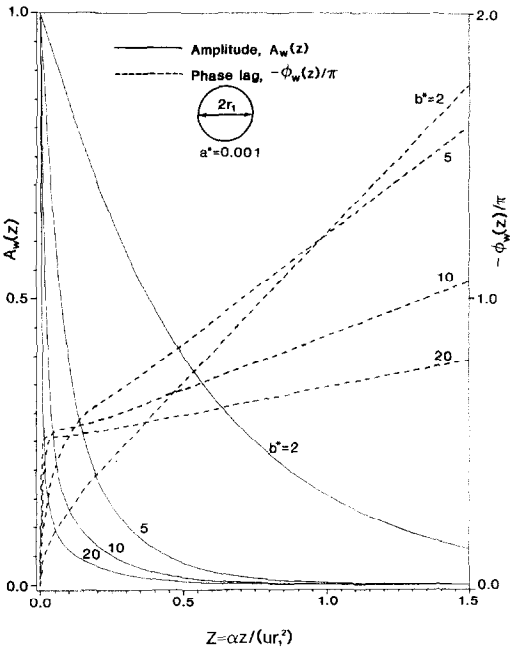

FIG. 1(b). Amplitude of phase lag for wall temperature as a function of the axial distance in a circular tube for various values of b^*.

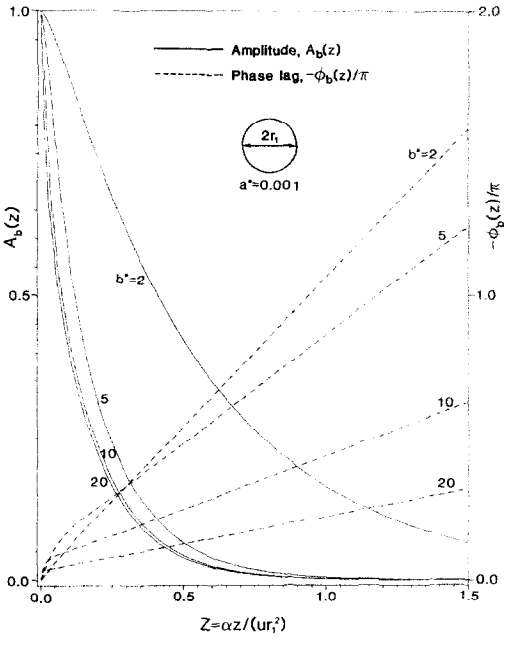

FIG. 2(b). Amplitude and phase lag for bulk temperature as a function of the axial distance in a circular tube for various values of b^*.

a metallic wall, the representative values of a^* are much smaller than unity. Therefore, we have chosen the values of a^* varying from 0.01 to 0.0005, for $b^* = 20$. We do not present results for small values of b^*, since the variation in a^* has little effect on both amplitude and phase lag. Note that, in Fig. 4, to the scale of the plot, the amplitudes are practically unchanged; the phase lags, however, seem to increase with increasing axial distance and the heat capacity ratio a^*. It seems that, the relatively large storage in the fluid itself 'delays' the information sensed by both wall and fluid. For small values of b^*, the storage in the wall being small, the system is rather insensitive to variations in the fluid storage.

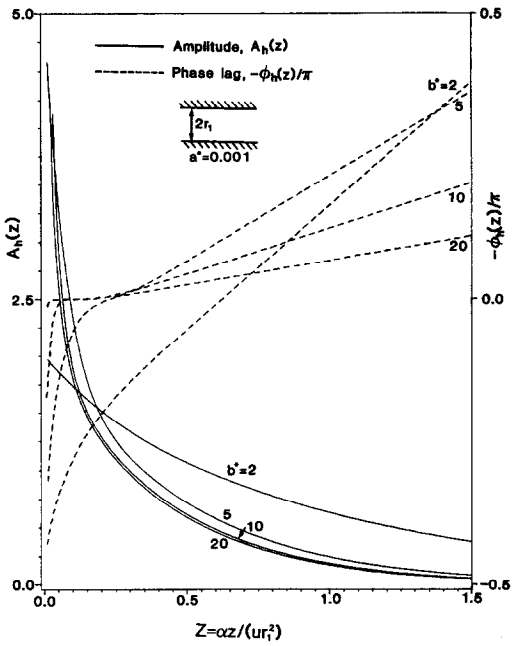

FIG. 3(a). Amplitude and phase lag for wall heat flux as a function of the axial distance in a parallel-plate channel for various values of b^*.

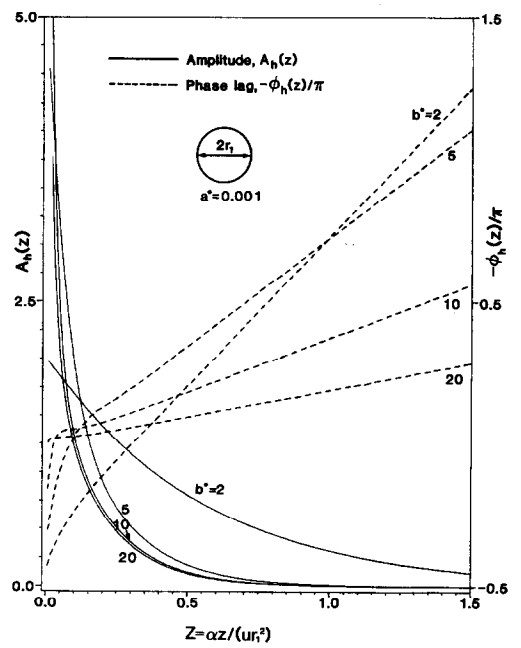

FIG. 3(b). Amplitude and phase lag for wall heat flux as a function of the axial distance in a circular tube for various values of b^*.

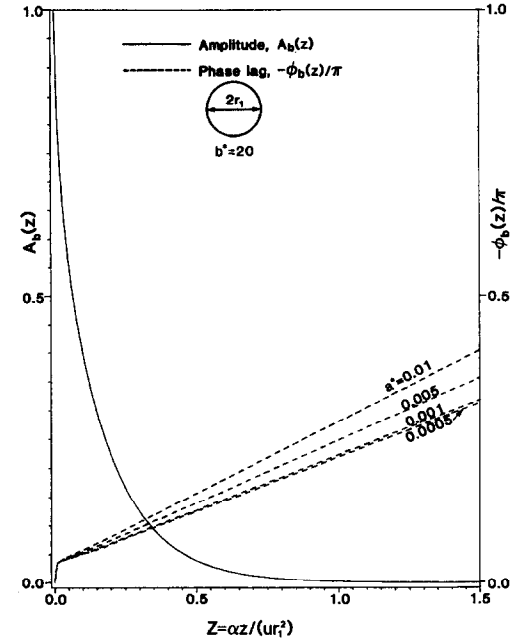

FIG. 4. Effects of the parameter a^* on amplitude and phase lag of the bulk temperature for flow inside a circular tube.

Acknowledgements—One of the authors (R.M.C.) wishes to acknowledge the financial support of Comissão Nacional de Energia Nuclear of Brazil. This work was also partially supported by the National Science Foundation through Grant No. Int-85-01097.

REFERENCES

1. E. K. Kalinin and G. A. Dreitser, Unsteady convective heat transfer and hydrodynamics in channels, *Adv. Heat Transfer* **6**, 367–502 (1970).
2. S. Kakaç and Y. Yener, Transient laminar forced convection in ducts. In *Low Reynolds Number Flow Heat Exchangers* (Edited by S. Kakaç, R. K. Shah and A. E. Bergles), pp. 205–227. Hemisphere, New York (1983).
3. E. M. Sparrow and F. N. de Farias, Unsteady heat transfer in ducts with time-varying inlet temperature and participating walls, *Int. J. Heat Mass Transfer* **11**, 837–853 (1968).
4. S. Kakaç and Y. Yener, Frequency response analysis of transient turbulent forced convection for timewise variation of inlet temperature. In *Turbulent Forced Convection in Channels and Bundles* (Edited by S. Kakaç and D. B. Spalding), Vol. 2, pp. 865–880. Hemisphere, New York (1979).
5. M. D. Mikhailov and M. N. Özişik, On the determination of the roots of some classes of transcendental equations, *Numer. Heat Transfer* **2**, 437–446 (1986).
6. M. D. Mikhailov and M. N. Özişik, *Unified Analysis and Solutions of Heat and Mass Diffusion*. Wiley, New York (1984).

CONVECTION VARIABLE, COUPLEE, FORCEE DANS DES CANAUX AVEC UNE TEMPERATURE VARIANT PERIODIQUEMENT A L'ENTREE DANS DES CANAUX

Résumé—La convection forcée variable pour un écoulement à deux plans parallèles ou circulaire, incluant couplage avec parois, est résolue analytiquement et exactement pour une variation périodique de la température d'entrée. La solution périodique du problème utilise des fonctions propres et des valeurs propres d'un problème complexe. Celui-ci est résolu en modifiant la récente méthode perfectionnée Count et les résultats sont présentés sous forme tabulaire des valeurs propres. L'amplitude et le retard de phase des oscillations, par rapport aux conditions à l'entrée sont déterminés pour la température pariétale, la température du fluide et le flux de chaleur. Les résultats pour les deux types de canaux sont présentés graphiquement en fonction de la position axiale pour différentes valeurs des paramètres signifiant le taux de stockage d'énergie dans les parois. On étudie les effets des parois sur l'amortissement de l'amplitude et l'altération de la phase des oscillations de température et de flux le long du canal.

INSTATIONÄRE GEKOPPELTE ERZWUNGENE KONVEKTION IN KANÄLEN MIT PERIODISCHER VARIATION DER EINTRITTSTEMPERATUR

Zusammenfassung—Die instationäre erzwungene Konvektion in Rechteckkanälen und kreisförmigen Rohren wird einschließlich der Anbindung an die Wand analytisch und exakt für eine periodische Variation der Eintrittstemperatur berechnet. Die periodische Lösung des Problems erfordert Eigenfunktionen und Eigenwerte eines komplexen Eigenwertproblems. Das komplexe Eigenwertproblem wird durch Modifikation der kürzlich verbesserten "Count-Methode" gelöst, und ausgewählte Ergebnisse für die Eigenwerte werden in Tabellenform dargelegt. Die Amplitude und die Phasenverschiebung von Schwingungen gegenüber dem Einrittszustand werden für die Wandtemperatur, die Fluidtemperatur und die Wärmestromdichte bestimmt. Die Ergebnisse für Rechteckkanäle und kreisförmige Rohre werden in graphischer Form als Funktion der axialen Lage für verschiedene Werte derjenigen Parameter, welche die Energiespeicherung in den Wänden darstellen, präsentiert. Der Einfluß der Wand auf die Dämpfung der Amplitude und die Phasenverschiebung der Temperatur- und Wärmestromschwingungen entlang des Kanals wird untersucht.

НЕСТАЦИОНАРНАЯ ВЫНУЖДЕННАЯ КОНВЕКЦИЯ В ТРУБАХ ПРИ ПЕРИОДИЧЕСКИ ИЗМЕНЯЮЩЕЙСЯ ТЕМПЕРАТУРЕ НА ВХОДЕ

Аннотация—Найдено точное аналитическое решение, включая сопряженную постановку задачи о нестационарной вынужденной конвекции для стержневого течения в плоскопараллельных каналах и круглых трубах. Периодическое решение задачи содержит собственные функции и собственные значения комплексной задачи на собственные значения. Решение получено с помощью модификации недавно предложенного метода счета. Полученные результаты для собственных значений приведены в таблицах. Определены амплитуда колебаний и их задержка по фазе по сравнению с условиями на входе для температуры стенки, среднеобъемной температуры жидкости и для теплового потока. Результаты, полученные для плоскопараллельных каналов и круглых труб, приведены в графическом виде как функции зависимости от положения на оси для различных значений параметров, определяющих скорость накопления энергии в стенках. Изучается влияние стенок на затухание амплитуды, а также изменение фазы колебаний температуры и теплового потока вдоль трубопровода.